Structural and Thermodynamic Characterization of the Interaction of the SH3 Domain from Fyn with the Proline-Rich Binding Site on the p85 Subunit of PI3-Kinase†

D. A. Renzoni,[‡,§] D. J. R. Pugh,[§,||] G. Siligardi,[⊥] P. Das,[#] C. J. Morton,[||] C. Rossi,[‡] M. D. Waterfield,[#] I. D. Campbell,[||] and J. E. Ladbury*[,||,○]

Oxford Centre for Molecular Science, University of Oxford, South Parks Road, Oxford OX1 3QT, U.K., Dipartimento di Chimica, Università di Siena, Pian dei Mantellini 44, 53100 Siena, Italy, National Chiroptical and Optical Spectroscopy Facility, Department of Pharmacy, King's College London, Manresa Road, London SW3 6LX, U.K., and Ludwig Institute for Cancer Research and Department of Biochemistry and Molecular Biology, University College London, 91 Riding House Street, London W1P 8BT, U.K.

Received August 20, 1996; Revised Manuscript Received October 14, 1996[⊗]

ABSTRACT: The interaction of the Fyn SH3 domain with the p85 subunit of PI3-kinase is investigated using structural detail and thermodynamic data. The solution structure complex of the SH3 domain with a proline-rich peptide mimic of the binding site on the p85 subunit is described. This indicates that the peptide binds as a poly(L-proline) type II helix. Circular dichroism spectroscopic studies reveal that in the unbound state the peptide exhibits no structure. Thermodynamic data for the binding of this peptide to the SH3 domain suggest that the weak binding (approximately 31 μM) of this interaction is, in part, due to the entropically unfavorable effect of helix formation ($\Delta S^\circ = -78$ J·mol^{-1}·K^{-1}). Binding of the SH3 domain to the intact p85 subunit (minus its own SH3 domain) is tighter, and the entropic and enthalpic contributions are very different from those given by the peptide interaction ($\Delta S^\circ = +252$ J·mol^{-1}·K^{-1}; $\Delta H^\circ = +44$ kJ·mol^{-1}). From these dramatically different thermodynamic measurements we are able to conclude that the interaction of the proline-rich peptide does not effectively mimic the interaction of the intact p85 subunit with the SH3 domain and suggest that other interactions could be important.

Src homology 3 (SH3)[1] domains are found in a large number of proteins which are involved in intracellular signal transduction and cytoskeletal composition. *In vivo* SH3 domains have been shown to bind to proline residue-rich regions of proteins, and they have been implicated in protein localization and regulation functions (Koch et al., 1991; Cicchetti, 1992; Ren, 1993). Most investigations of the binding properties of SH3 domains have been focused solely on the proline-rich motifs themselves due to the convenience of using a peptide rather than an intact protein. Structures of complexes between SH3 domains and short peptides revealed that these proline-rich motifs bind in the form of poly(L-proline) type II (PPII) helices (Kuriyan & Cowburn, 1993, and references therein; Mussachio et al., 1994; Feng et al., 1994; Goudreau et al., 1994; Lim et al., 1994; Terasawa et al., 1994; Yu et al., 1994). Specificity appeared to be based on recognition of residues other than proline that are interspersed in the proline-rich sequence (Lim & Richards, 1994; Sparks et al., 1994; Yu et al., 1994; Alexandropoulos et al., 1995) and enhanced by immediately surrounding residues (Rickles et al., 1994, 1995; Feng et al., 1995). An additional level of specificity may be derived from the ability of different peptides to bind in two opposing orientations (Feng et al., 1994; Lim et al., 1994; Wu et al., 1995). Binding studies (Viguerra et al., 1994; Cussac et al., 1994; Lemmon et al., 1994; Wittekind et al., 1994) show that the interactions of peptides with SH3 domains are typically weak (10^{-4}−10^{-5} M).

The large number of intracellular proteins found bearing proline-rich motifs suggests that there should be a range of specificity or selectivity in SH3−protein interactions. SH3−peptide interactions, as explored by peptide mimics of physiological ligands, show such low affinity that the issue of specificity is called into question. Deletion experiments on the established ligand for the SH3 domain from Abl revealed that proline-rich motifs could bind in isolation to the SH3 domain but with lower affinity than the whole protein or larger polypeptides derived from the protein (Cicchetti et al., 1992; Ren et al., 1993). Tighter binding than represented by peptide interactions has been observed in the binding of the SH3 domain from Hck with the intact HIV-1 Nef protein, which was attributed to selective recognition of a region proximal to the proline-rich region

† D.J.R.P. is a Wellcome Trust Mathematical Biology Fellow and J.E.L. is Wellcome Trust Research Career Development Fellow. We thank the Wellcome Trust and Zeneca for support for I.D.C. and C.J.M., respectively. The OCMS is funded by the BBSRC, MRC, and EPSRC. The NCOSC is funded by the EPSRC and ULIRS.

* Address correspondence to this author.
‡ Università di Siena.
§ Authors contributed equally to this work.
|| University of Oxford.
⊥ King's College London.
University College London.
○ Present address: Department of Biochemistry and Molecular Biology, University College London, 91 Riding House St., London W1P 8BT, U.K.

⊗ Abstract published in *Advance ACS Abstracts,* November 15, 1996.

[1] Abbreviations: SH3, Src homology domain 3; NMR, nuclear magnetic resonance; ITC, isothermal titration calorimetry; CD, circular dichroism; ΔSH3p85, SH3-deleted p85 subunit of PI3-kinase; P2L, proline-rich peptide derived from the p85 subunit of PI3-kinase; PPII, poly(L-proline) type II helix; GST, glutathione *S*-transferase; NOE, nuclear Overhauser effect; NOESY, NOE spectroscopy; DQF-COSY, double-quantum-filtered correlation spectroscopy; TOCSY, total correlation spectroscopy.

S0006-2960(96)02096-X CCC: $12.00

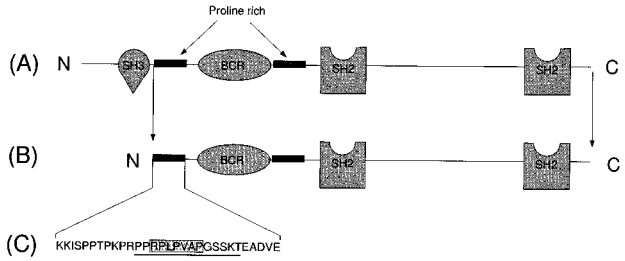

FIGURE 1: Schematic representation of (A) the complete p85 subunit from PI3-kinase indicating the positions of domains and proline-rich sequences, (B) the ΔSH3p85 protein used in the binding studies, and (C) the 30-residue N-terminal proline-rich sequence with the peptide used in this work (underlined) and the seven residues involved in interaction with the SH3 domain (shaded).

of the protein by an isoleucine in the SH3 RT loop [Lee et al., 1995; reviewed by Lim (1996)]. This indicated that additional interactions other than those with the proline-rich region were important.

Here we present further evidence that physiological interactions of SH3 domains in some cases are not adequately represented by data derived from binding of proline-rich peptide mimics of protein binding sites. To investigate this issue, it is necessary to characterize the interaction of an SH3 domain with peptide and to compare these data to those obtained for the interaction with the same sequence of residues which are within a protein. We achieved this by determining the structural−thermodynamic relationship for the interaction of the Fyn SH3 domain with a peptide mimic (P2L) proline-rich region corresponding to residues 91−104 of the p85 subunit and with the whole p85 subunit of PI3-kinase. Fyn, a member of the Src family of tyrosine kinases, plays a role in intracellular signal transduction via interaction with the T-cell receptor complex. The SH3 domain of Fyn has been shown to be involved in the recruitment of the p85 subunit of PI 3-kinase (Kapellar et al., 1994) via interaction with a proline-rich sequence (Figure 1). It has been suggested that the p85 subunit is able to regulate the binding of the Fyn SH3 domain by the interaction of its own SH3 domain (situated at the N-terminus) with the proline-rich region between this domain and the BCR domain (Figure 1; Kapeller et al., 1994; Pleiman et al., 1994). To avoid any effects from intramolecular or intermolecular (homodimer formation) interaction in this study, the SH3 domain of the p85 subunit was deleted to produce ΔSH3p85 (Figure 1B).

From the data described in this work it is apparent that the peptide binds with an affinity consistent with other reported SH3−peptide interactions but is likely to bind in a thermodynamically very different way to the proline-rich region within the ΔSH3p85. The components of the free energy of the interactions reveal that in the peptide interaction a negative entropic effect is observed, whereas with the ΔSH3p85 the entropic contribution is favorable. Since the proline-rich binding site is likely to be folded into a PII-type helical conformation in the physiological ligand, the dramatic entropic effects are likely to result at least in part from the formation of the PII helix from the peptide. From the detailed structural and thermodynamic data we suggest that significant additional interactions outside the realm of the SH3−peptide interface are important.

EXPERIMENTAL PROCEDURES

Preparation of SH3 Domain. The SH3 domain used in this work corresponds to residues 82−148 of the intact Fyn protein. The domain in all cases was expressed fused with glutathione *S*-transferase (GST). The GST was cleaved for all experiments except for the isothermal titration calorimetric studies. There was no apparent effect due to the presence of GST in these calorimetric experiments as has been previously demonstrated (Ladbury et al., 1995). Expression in *Escherichia coli* BL21 cells in pGEX-2T plasmid (a kind gift from Dr. C. Rudd), thrombin cleavage of the GST fusion, and purification of both the ^{15}N-labeled and unlabeled SH3 domain has been described elsewhere (Morton et al., 1996). The SH3 domain was buffer exchanged (Bio-Rad DG10 columns) into 10 mM phosphate buffer, pH 6.0. All subsequent experiments were performed in this buffer system. The polypeptide solutions were concentrated (Centriprep and Centricon, Amicon) where appropriate. Purity and composition of the samples were confirmed by SDS−PAGE and electrospray mass spectroscopy. SH3 domain concentrations were assessed by optical density [the extinction coefficient at 280 nm (ϵ_{280}) for the SH3 domain = 16600 $M^{-1}\cdot cm^{-1}$; ϵ_{280} for the GST−SH3 domain = 59900 $M^{-1}\cdot cm^{-1}$) and by amino acid analysis.

Preparation of ΔSH3p85. The sequence chosen corresponds to the region 79−724 of the p85 subunit of human PI3-kinase shown schematically in Figure 1B (Skolnik et al., 1991). The construct was expressed as a GST fusion from a pGEX-2T vector in *E. coli* BL21 cells. Thrombin cleavage and purification were performed as described for the SH3 domain above (Morton et al., 1996). The purity of the expressed protein was assessed by SDS−PAGE, and concentrations were assessed by optical density (ϵ_{280} for ΔSH3p85 = 77600 $M^{-1}\cdot cm^{-1}$) and by amino acid analysis.

Preparation of Peptide. The 14-residue peptide (P2L), with the amino acid sequence PPRPLPVAPGSSKT corresponding to residues 91−104 of the p85 subunit (Figure 1C), was synthesized as described elsewhere (Ladbury et al., 1996). High-performance liquid chromatography was used to purify the peptide. The peptide was lyophilized prior to resuspension in the buffer system described above. The purity of the peptide was confirmed by electrospray mass spectroscopy, and concentrations were assessed by mass and amino acid analysis.

Nuclear Magnetic Resonance Spectroscopy and Structural Calculations. Spectra were recorded at 500, 600, and 750 MHz on custom-built instruments described elsewhere (Morton et al., 1996). 2-D ^{1}H−^{1}H DQF-COSY (Rance et al., 1983), ^{1}H-^{1}H TOCSY (Braunschweiler & Ernst, 1983), and ^{1}H−^{1}H ROESY (Bax et al., 1985) spectra allowed the unambiguous sequential assignment of the spin systems of the unliganded peptide in 90:10 H_2O:^2H_2O (v/v). For the structural determination of the complex, SH3 domain samples were prepared as described above [with 5% ^2H_2O (v/v)] with a 4-fold molar excess of peptide added prior to use.

Assignment of the spin systems and measurement of intra-SH3 NOEs of the SH3 domain in the complex were facilitated by comparison of 2-D ^{1}H−^{1}H TOCSY and NOESY spectra of the liganded and unliganded (Morton et al., 1996) SH3 domain. Careful analysis of chemical shift changes, NOE, and $^3J_{HN-H\alpha}$ coupling data indicates that the conformation of the SH3 domain does not change signifi-

cantly on going from the free to complexed form. This being the case, for residues not involved in binding, NOE-derived constraints from free Fyn SH3 were used in the structural calculation. Intermolecular NOEs, as well as intra-SH3 NOEs for residues involved in binding, were collected from ^{15}N-coupled and -decoupled ^{1}H$-^{1}$H NOESY spectra (mixing time 150 ms) recorded at 30 °C. These were graded into three groups, strong, medium, and weak, and apportioned upper limit distance constraints of 2.8, 3.5, and 5.0 Å respectively. Lower limit distance constraints were taken to be the sum of the van der Waals distances for all atoms. To account for additional intensities from unresolved protons, constraints involving methyl groups were corrected by a constant (0.5 Å per group). A 2-D ^{1}H$-^{15}$N HMQC-*J* spectrum was recorded from which the $^{3}J_{\mathrm{HN-H\alpha}}$ coupling constants of the SH3 domain in the complex were extracted.

All structural calculations were carried out using X-PLOR 3.1 (Brünger, 1992). A total of 100 random peptide structures were generated, and each was docked, on the basis of two NOE-derived constraints, onto the representative unbound SH3 structure which was kept fixed. The atoms of the SH3 domain were then freed, and the whole complex was subjected to repeated rounds of simulated annealing using the full set of intermolecular and intra-SH3 distance constraints. All peptide bonds were constrained to be in the *trans* conformation, and no electrostatic terms were included in the target energy function. The final value of k_{repel} used was 0.75. $^{3}J_{\mathrm{HN-H\alpha}}$ coupling constants were used to derive constraints for the backbone torsional angle, ϕ, as described elsewhere (Morton et al., 1996). Hydrogen bonds previously identified in the unliganded SH3 domain were included only between atoms in regions unaffected by the presence of the peptide.

One hundred final structures were obtained from which the 25 with lowest energy were selected. The root-mean-square deviation (RMSD) of the family was determined by taking the average of the RMSDs of the individual structures from the set of mean coordinates after superimposing the structures using a least-squares fit. A representative structure was generated using the "probability map refinement" method described elsewhere (DeLano & Brünger, 1994).

Circular Dichroism Spectroscopy (CD). CD spectra were recorded using a nitrogen-flushed JASCO spectropolarimeter J720 using a 4 s time constant, 10 nm·min^{-1} scan speed, and 1 nm spectral bandwidth. A 1 cm path-length cell was used for the near-UV CD region (240−320 nm) and a 0.02 cm cell was used for the far-UV CD region (185−260 nm) as depicted in Figure 2. All spectra were recorded in buffer conditions described above except for the low temperature analysis, in which case 2:1 ethanediol−water (v/v) was used as the solvent. CD spectra of the bound P2L peptide at different molar ratios were obtained by subtracting the CD spectrum of the free SH3 domain from the spectra of the SH3/P2L mixtures with the assumption that there are no structural changes in the SH3 domain. CD data were analyzed using the MathCad (Drake, unpublished) program assuming a stoichiometry of 1:1 P2L ligand:SH3 domain.

The 14-residue P2L peptide contains no aromatic residues and hence exhibits no CD signal in the near-UV region. The SH3 domain has three Phe, four Tyr, and two Trp residues which show a broad positive band (250−300 nm). Two strong components at approximately 295 and 285 nm are characteristic of the Trp residues. On addition of P2L

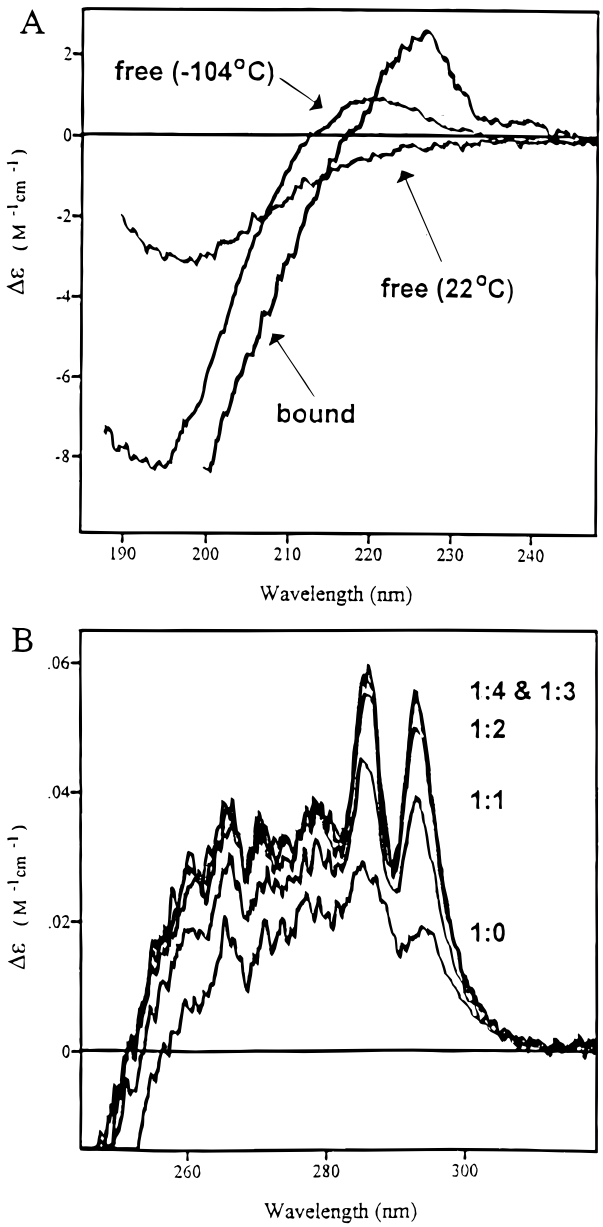

FIGURE 2: (A) CD spectroscopic analysis of P2L peptide conformation. The figure shows three independently determined spectra: the spectrum for the free peptide at 22 °C suggesting that there is no secondary structure present; the spectrum of P2L peptide bound to the Fyn SH3 domain in a 1:1 concentration ratio with the spectrum of the free SH3 domain subtracted; the spectrum of free P2L peptide at −104 °C showing PPII helical conformation. (B) CD spectra in the Trp absorbance region for the binding of P2L peptide to the SH3 domain from Fyn obtained at 30 °C. The $\Delta\epsilon$ at 293 nm was measured as a function of concentration from which a dissociation constant of 28 μM for the interaction was obtained.

peptide to the SH3 domain the intensity of the aromatic side chain-derived signal increases, indicative of a reduction in their mobility and local environmental changes on binding (Figure 2B). This change in intensity on addition of peptide to SH3 enabled the dissociation constants, K_{D}, to be determined. This was achieved by measuring the $\Delta\epsilon$ value at 293 nm for a range of concentrations and best-fitting this for K_{D} as described elsewhere (Strickland, 1974).

Isothermal Titration Calorimetry (ITC). All experiments were performed using the MCS system (MicroCal Inc., MA) as described elsewhere (Wiseman et al., 1989; Ladbury, 1996). In a typical experiment 1.75 mM P2L peptide was added in 20 12-μL injections to a 0.09 mM solution of

the Fyn SH3 domain in the 1.3-mL calorimeter cell at 30 °C. The resulting data were fit as described elsewhere (Wiseman et al., 1989) after subtracting the heats of dilution, resulting from addition of peptide into buffer and buffer into SH3 domain, determined in separate control experiments. Titration data were fit using a nonlinear least-squares curve-fitting algorithm with three floating variables: stoichiometry, binding constant ($K_B = 1/K_D$), and change of enthalpy of interaction ($\Delta H°$). ITC gives a complete thermodynamic characterization of an interaction based on the equation:

$$-RT \ln K_B = \Delta G° = \Delta H° - T\Delta S°$$

where R is the gas constant, T is the absolute temperature, and $\Delta G°$, $\Delta H°$, and $\Delta S°$ are the standard free energy, enthalpy, and entropy changes on going from unbound to bound states, respectively.

Reported data are derived from the mean of three titrations, and the errors are assessed by standard deviation as follows: for the P2L−SH3 interaction K_D is ± 1 μM and $\Delta H°$ is $\pm$ 0.1 kcal·mol^{-1}; for the ΔSH3p85−SH3 interaction K_D is $\pm$ 1 μM and $\Delta H°$ is $\pm$0.4 kcal·mol^{-1}.

RESULTS

To completely define the structural and thermodynamic relationship for the binding of the proline-rich peptide to the SH3 domain from Fyn, it is necessary to characterize the structure of the components of the interaction in both free and bound states.

Conformation of the Unbound Peptide. Reported data on free proline-rich peptides that are recognized by SH3 domains suggested that they can possess some structure (Viguera et al., 1994). Poly(L-proline) is able to form two distinct structures in isolation, a *cis*-imide conformation in a right-handed helix with 3.3 residues per turn (PPI) and a left-handed helix of *trans*-imide groups with three residues per turn (PPII). The PPII secondary structure has an axial translation of 3.12 Å per residue ($\phi = -75°$, and $\psi = 145°$). Both NMR and CD spectroscopy were used to determine whether these, or any other conformation, were present in the proline-rich unbound peptide.

NMR analysis provides no evidence of short- or long-range NOE interactions in the free peptide. While ruling out other forms of secondary structure, this does not remove the possibility of formation of PPII helix structure because analysis of this structure shows that there are no observable NOEs characteristic of this conformation. In addition, it should be noted that the ϕ angles in PPII give rise to expected $^3J_{HN-H\alpha}$ coupling constants in the range 5−8 Hz; these values give multiple solutions to the Karplus equation (Karplus, 1959) and could arise from rapid conformational averaging.

CD spectroscopy provides a method to determine the presence of elements of secondary structure in the peptide. PPII helices have distinct absorbance of circularly polarized light in the region of 217−226 nm (Siligardi & Drake, 1995). The free peptide shows no evidence of PPII helix (Figure 2A). The featureless CD spectrum is consistent with the free peptide being nonstructured. Evidence of structure in proline-rich peptides, previously reported (Viguera et al., 1994), was not observed in our CD spectra even in the presence of trifluoroethanol (TFE), which can induce α-helical or β-turn conformation (Waterhous & Johnson, 1994). The peptide does, however, have the ability to form a PPII conformation in isolation at low temperature. At −104 °C a positive peak centered at approximately 220 nm in the region associated with the left-handed extended PPII helix conformation (Drake et al., 1988) is observed (Figure 2A). Under conditions of reduced entropy at low temperature, the helical conformation of the peptide becomes more favorable (Drake et al., 1988).

Structure of the Unbound SH3 Domain. The crystal (Noble et al., 1993) and solution (Morton et al., 1996) structures of the unbound Fyn SH3 domain have been solved and reported previously. The structure is typical of SH3 domains, comprising a compact β-barrel of six β-strands and a single turn of a 3_{10} helix. In this work we restrict all further discussion of the unbound SH3 domain of Fyn to data obtained from the solution structure of Morton et al. (1996).

Solution Structure of the Complex. In a previous study a model for the complex was proposed on the basis of the above unbound SH3 domain structure with the peptide, which was assumed to adopt a PPII helix conformation (Morton et al., 1996). In this earlier work the structure of the complex was determined by constraining the peptide in the PPII helical form and docking it onto a fixed SH3 structure using just 15 NOEs. In the current work we report the solution structure of the Fyn SH3 domain in complex with the 14-residue P2L peptide, using dynamic simulated annealing, making no *a priori* assumptions about the peptide conformation.

A total of 629 structurally significant NOE-derived distance constraints [as assessed by the program DIANA (Guntert et al., 1991)] were used in the calculation of the structure, as described in Experimental Procedures. These include 50 intermolecular and 579 intra-SH3 constraints, as well as 42 constraints for 21 intra-SH3 hydrogen bonds and 35 intra-SH3 backbone ϕ angle constraints. The 579 intra-SH3 constraints are made up of 103 intraresidue, 135 sequential, 54 short-range ($1 < |i - j| < 5$), and 287 long-range ($|i - j| \geq 5$) interactions. The N-terminus (residues 82 and 83) and C-terminus (residues 142−148) of the SH3 domain showed no structurally significant NOEs, and hence these residues were excluded from the calculations. With regard to the peptide no structural information was obtained through intrapeptide NOEs (hence no distance constraints were imposed on the peptide), and residues 1−2 and 10−14 were excluded from the final structural calculations because no intermolecular NOEs were observed.

A superposition of the backbone traces of the final 25 structures of the complex is shown in Figure 3, and a summary of the data obtained can be found in Table 1. None of the structures have distance constraint violations greater than 0.1 Å or dihedral angle violations greater than 0.5°. The average RMSD of the 25 final structures relative to their mean coordinates is 0.63 $\pm$ 0.13 Å for all backbone atoms and 1.16 $\pm$ 0.12 Å for all heavy atoms. Residues 114−118 of Fyn SH3 appear to be relatively unstructured; excluding these residues from the calculation, the RMSD is 0.57 $\pm$ 0.13 Å for backbone atoms and 1.10 $\pm$ 0.08 Å for heavy atoms.

The structure is in good agreement with those of previous proline-rich peptide−SH3 domain interactions (Feng et al., 1994). Proline-rich peptides binding to SH3 domains have been observed to adopt one of two possible orientations ("plus" or "minus") based on steric constraints and electrostatic interactions (Feng et al., 1994; Lim et al., 1994). The

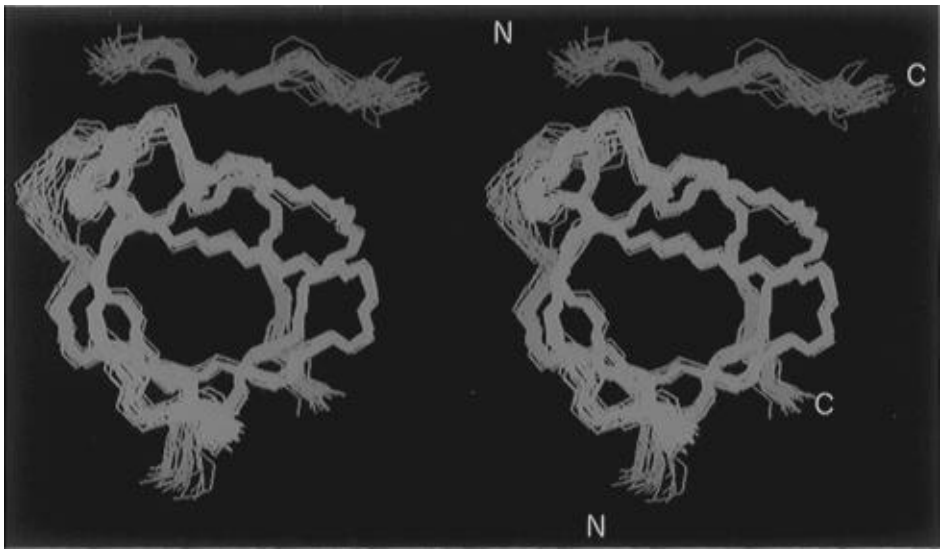

FIGURE 3: Stereoview of a superimposition of the 25 final structures of the backbone atoms of the complex of the SH3 domain from Fyn (green) in complex with P2L peptide (interacting residues 3−9 shown in magenta).

Table 1: Structural Statistics of the Family of 25 Fyn SH3−P2L Peptide Structures and the Representative Structure[a]

structural property	NMR family	representative structure
NOE-derived constraints (Å)		
all (629)	0.0063 (7)	0.0068
intermolecular SH3−P2L (50)	0.0053 (24)	0.0050
long range in SH3 (287)	0.0042 (8)	0.0020
short range in SH3 (54)	0.0049 (33)	0.0024
sequential in SH3 (135)	0.0058 (17)	0.0111
intraresidue in SH3 (103)	0.0097 (25)	0.0103
other experimental constraints		
hydrogen bond lengths (42) (Å)	0.0078 (28)	0.0032
ϕ constraints (35) (deg)	0.031 (32)	0.000
idealized geometry[b]		
ideal bond lengths (Å)	0.00267 (3)	0.00258
ideal angles (deg)	0.605 (3)	0.570
impropers (deg)	0.239 (4)	0.216

[a] Values quoted are RMS deviations from experimental or idealized data. [b] Comparison with the idealized geometry used by X-PLOR 3.1. Numbers in parentheses in the left-hand column are the numbers of constraints in each category.

P2L peptide adopts a helical PPII-like conformation between residues 5 and 9 and binds in the plus orientation. Residues 3 and 4 are also likely to form PPII helical structure both because of the proline-rich environment in which they are found and because no further structural violations are observed on imposing the corresponding dihedral angle constraints on these two residues in structural calculations; however, unequivocal evidence for this could not be obtained. In the peptide the critical prolines (residues 6 and 9) interact with binding pockets PII and PIII, respectively, while Leu 5 and Ala 8 bind in pockets PV and PIV, respectively [nomenclature derived from Feng et al. (1994)]. We find no direct evidence for a salt bridge between Arg 3 in the peptide and Asp 100 in the SH3 domain; however, constraining the structures to satisfy the conditions for salt bridge formation leads to no additional close contacts that would be detected in our NMR data or cause violations of the existing experimental constraints. Experimental evidence, therefore, is consistent with the presence of a salt bridge in this position.

CD spectroscopic studies of the free and complexed molecules provided further evidence that the P2L peptide adopts a PPII structure on binding. As mentioned above, the positive peak associated with the PPII helix is found in the spectral region from 217 to 226 nm depending on the proline content of the peptide. Studies on model peptides show that as the proline content of peptides is increased, the positive CD band shifts to higher wavelengths in this region. The maximum wavelength (λ_{max}) for the bound peptide (see Experimental Procedures) was observed at 226 nm whereas λ_{max} for the free peptide at low temperature (see above) is at 220 nm (Figure 2A). These data suggest that at low temperature we are observing a signal corresponding to the whole peptide in the PPII form (proline content 36%) while in the complex only the more proline-rich N-terminal region of the peptide is adopting the PPII helix (proline content 56%). This is consistent with the NMR spectroscopic data.

Table 2: Thermodynamic Data from the Binding Studies of Fyn SH3 with both P2L Peptide and ΔSH3p85 at 30 °C (303.15 K)

	K_D (μM)	$\Delta G°$ (kJ·mol^{-1})	$\Delta H°$ (kJ·mol^{-1})	$\Delta S°$ (J·mol^{-1} K^{-1})
SH3 Domain + P2L Peptide				
NMR[a]	50	−25.0		
CD	28	−26.4		
ITC	16	−27.8	−51.4	−77.8
SH3 Domain + p85 Subunit of PI3-Kinase				
ITC	3	−32.0	+44.3	+251.7

[a] Morton et al. (1996).

Affinity of Interaction of P2L Peptide with the SH3 Domain. The binding of the peptide to the SH3 domain was investigated using NMR, CD, and ITC at 30 °C (Table 2). Despite the quite different methods the binding data are in good agreement. Using these very different probes of binding the average K_D is found to be of the order of 31 μM, giving a free energy $\Delta G°$ for the interaction of −26 kJ·mol^{-1}. This value is typical of those previously obtained for peptide−SH3 interactions and represents a fairly weak interaction. Calorimetric data enable the determination of the entropic and enthalpic components of free energy (ΔS° and $\Delta H°$, respectively). The calorimetrically determined $\Delta G°$ for the interaction of the peptide with the SH3 domain is −28 kJ·mol^{-1}. This interaction is characterized by a large,

unfavorable entropic contribution to the binding ($\Delta S° = -78$ J·mol^{-1}·K^{-1}). This observation is in agreement with data for the interaction of the SH3 domain from Grb2 with a peptide derived from murine Sos-2 (Wittekind et al., 1994). Unfavorable entropic effects are derived from the reduction of the degrees of freedom of the system. Components of this are derived from several sources including the formation of structural elements, the restriction of vibrational modes of interatomic bonds by an overall "tightening" of the structure, and the restriction of water molecules into an interface (Morton & Ladbury, 1996).

The entropic contribution to free energy is opposed and dominated by a large favorable enthalpic effect. The enthalpy is the sum of exothermic and endothermic contributions derived from the formation or removal of noncovalent interactions, respectively.

The relationship between the structural and thermodynamic information for the binding of the P2L peptide to the SH3 domain derived from NMR, CD, and ITC methods enables us to better understand the interaction. On formation of the complex the SH3 domain shows no significant structural alteration; however, the peptide undergoes a change from being nonstructured to being partially structured in a PPII-type helix. This process is likely to incur a significant entropic penalty and undoubtedly accounts for some of the unfavorable contribution to the observed $\Delta G°$. Other possible contributions to the unfavorable entropy are not obvious, apart from the possible reduction in side chain mobility of the amino acids in the SH3 binding site, as confirmed by CD and ^{15}N NMR relaxation data (data not shown). There is also no evidence for the inclusion of water molecules into the highly hydrophobic interface, and none have been reported in crystallographic analysis (Musacchio et al., 1994; Lim & Richards, 1994). There are no obvious hydrogen bonds formed between the SH3 domain and the peptide seen in the NMR structural data, indicating that the favorable enthalpy is likely to result from the formation of hydrophobic contacts. Site-directed mutagenesis experiments indicate that a salt bridge is very likely to be formed between the Arg of the proline-rich peptide and a highly conserved acidic residue in the SH3 domain (Yu et al., 1994). The presence of such a salt bridge is consistent with our structural data although, as described above, we have no direct evidence for its existence. Some unfavorable enthalpic contribution will inevitably result from the breaking of weak hydrogen bonds formed between ordered water molecules on the hydrophobic surfaces of both the SH3 domain and the peptide.

Binding of the SH3 Domain to the ΔSH3p85 Protein. To demonstrate the differences between the interaction of peptide mimics and physiological ligands, the binding of the SH3 domain to the ΔSH3p85 protein was studied by ITC at 30 °C. The ΔSH3p85 protein used has two proline-rich regions, one immediately N-terminal and one C-terminal of the BCR domain (Figure 1). Fyn has been shown to recognize only the residues in the N-terminal sequence found within the P2L peptide (Pleiman et al., 1994). This has been verified by selection from random peptide libraries (Ladbury and Morton, unpublished data) and by peptide binding studies (Morton et al., 1996). In our binding a stoichiometry of 1:1 is observed which can safely be assumed to represent the binding of the SH3 domain to the region ΔSH3p85 with the P2L sequence. No additional binding was observed. Table 2 shows the thermodynamic parameters associated with the binding of both peptide and protein. The binding of the ΔSH3p85 is tighter than the binding of the peptide to the SH3 domain (average K_D incorporating NMR, CD, and ITC data is approximately an order of magnitude tighter, whereas taking the ITC data alone gives a 5-fold increase in affinity). It is immediately obvious on comparing the two that the entropic and enthalpic components of the free energy are vastly different; indeed, they are of opposite signs.

DISCUSSION

The structural and thermodynamic relationship for the binding of a peptide derived from the p85 subunit of PI3-kinase (P2L) has been investigated. This has been based on detailed solution structural information and accurate thermodynamic data to characterize the closed system represented in Figure 4A. The affinity for this interaction is in the range previously observed for SH3−peptide. The data show that whereas the structure of the SH3 domain is unchanged, the peptide goes from an unstructured form to a PPII-type helix upon binding (Figure 4A). This conformational change of one of the components in the absence of any other significant source is largely responsible for the unfavorable entropy of this interaction. Thus the effect of folding the peptide into the helix upon binding is to reduce the observed affinity. The favorable enthalpic effect is likely to be derived from van der Waals-type interactions on burial of hydrophobic surface area in the binding interface (Figure 4B), this enthalpic gain being greater than any cost of removal of interacting water on the unbound hydrophobic surfaces of the free peptide and SH3 domain.

The binding of the Fyn SH3 domain to the ΔSH3p85 protein, which is a far better model of one defined physiological interaction of the p85 subunit, gives entirely different thermodynamic data than in the formation of the peptide complex. The affinity of the interaction with the ΔSH3p85 is tighter, giving rise to about 4 kJ·mol^{-1} reduction in the $\Delta G°$. This is slightly tighter than the interaction of the SH3 domain of Fyn with Nef described by Lee et al. (1995).

The dramatic reversal of the entropic and enthalpic components of $\Delta G°$ is remarkable. In the absence of structural information of the SH3−ΔSH3p85 complex we can only speculate on the causes of this effect. It is likely that the proline-rich motif (represented by the P2L peptide) in the context of the p85 protein subunit is, at least partly, in the form of a PPII-type helix. It might be expected that in the regulation mechanism mentioned above the proline-rich binding site on p85 for the p85 SH3 domain is presented in its folded form with a flexible loop linking the two. It is anticipated that the cleavage site to give ΔSH3p85 (residue 79) is in the loop region distal from the proline-rich site (starting at residue 91). In addition, proline-rich binding sites have been shown to have helical conformation in the structural studies of Nef (Grzesiek et al., 1996) and its complex with the Fyn SH3 domain (Lee et al., 1996). The proline-rich helix of Nef is stabilized by interactions with other regions of the protein. If the proline-rich motif is already folded, the entropic cost of the formation of the helix required for the unstructured free peptide is removed.

A positive entropic contribution to the $\Delta G°$ could be derived from the removal of "ordered" water by the burial of additional hydrophobic surface area on top of that in the

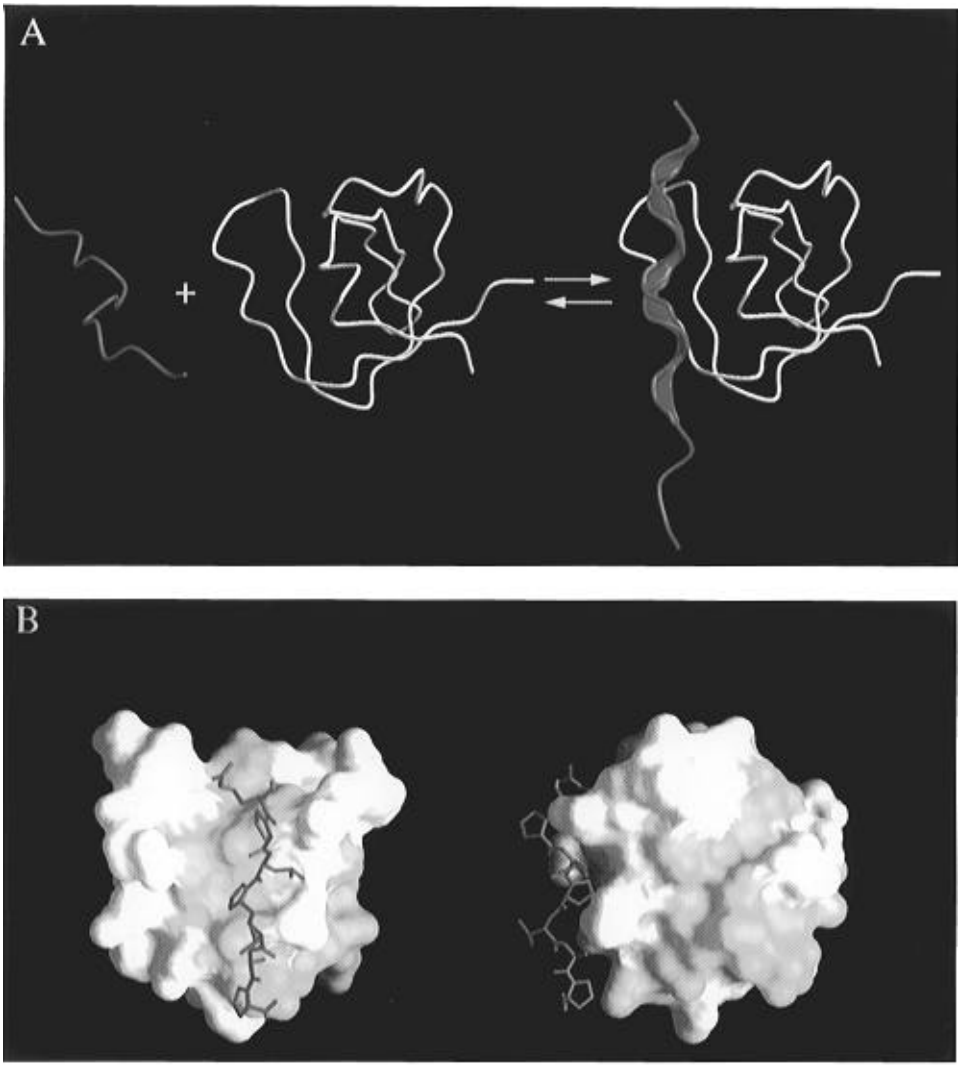

FIGURE 4: (A) Schematic structural representation of the thermodynamic closed system of the peptide−SH3 interaction investigated in this work. (B) Views of the P2L peptide (green) binding to an accessible surface representation of the Fyn SH3 domain. Trp, Tyr, and hydrophobic residues are shown in yellow. The surface was calculated from the representative complex structure using the GRASP program (Nicholls et al., 1991). The figure on the left shows the P2L helix binding to a hydrophobic site on the SH3 domain. The figure on the right is a 90° clockwise rotation around the vertical axis of the figure on the left and shows large regions of hydrophobic surface area proximal to the peptide binding site (in yellow).

binding of the P2L peptide. Figure 4B shows the binding face of the SH3 domain with hydrophobic surface colored. Although the interaction with the proline-rich region represented by the P2L peptide covers some of this, there is clearly additional proximal surface that could be involved with a more extensive interface on p85. Indeed, the peptide interaction covers less than a sixth of the total hydrophobic surface area of the SH3 domain. The unfavorable enthalpic effect of the ΔSH3p85 interaction could thus be the result of the breaking of bonds in the surface water. This enthalpic loss is not recovered from interactions made between the interacting protein molecules. Our data, thus, might suggest a much larger binding site than that represented by the SH3−P2L interaction. Another source of the dramatic change in binding properties between the peptide and the protein could be derived from gross conformational changes to the protein structure (such as reorientation of the various domains) on binding.

The recently reported structure of the complex between a mutated Fyn SH3 domain, (R96I)SH3, and Nef provides a useful context for comparison with our data (Lee et al., 1996). The Fyn−Nef structure describes additional interactions other than those formed with the peptide. The most important of these additional interactions is via the RT loop, which appears to impart another level of specificity. This interaction involves the burial of a hydrophobic surface area in a pocket formed by two antiparallel α-helices close to the PPII-type helix. The thermodynamics of binding of the (R96I)SH3 domain with Nef are very different from those we obtain for the SH3/ΔSH3p85 interaction, indicating that significantly different interactions are made. Nonetheless, the evidence for additional interactions between the SH3 domain and ΔSH3p85 other than that represented by the P2L peptide interaction, although circumstantial, is compelling. Further detail awaits structural determination of the complex. It is, however, quite clear from the thermodynamic data that the interaction of the P2L peptide is significantly different from the interaction with the physiological ligand.

ACKNOWLEDGMENT

The authors thank Drs. T. Mulhern, J. Werner, G. Shaw, and R. O'Brien for their discussion and comments on the manuscript.

REFERENCES

Alexandropoulos, K., Cheng, G., & Baltimore, D. (1995) *Proc. Natl. Acad. Sci. U.S.A. 92*, 3110−3114.

Bax, A., & Davis, D. G. (1985) *J. Magn. Reson. 63*, 207−213.

Braunschweiler, L., & Ernst, R. R. (1983) *J. Magn. Reson. 53*, 521−528.

Brünger, A. T. (1992) *X-PLOR Manual, Version 3.1*, Yale University, New Haven, CT.

Cicchetti, P., Mayer, B. J., Thiel, G., & Baltimore, D. (1992) *Science 257*, 803-806.

Cussac, D., Frech, M., & Chardin, P. (1994) *EMBO J. 13*, 4011−4021.

DeLano, W. L., & Brünger, A. T. (1994) *Proteins: Struct., Funct., Genet. 20*, 105−123.

Drake, A. F., Siligardi, G., & Giggons, W. A. (1988) *Biophys. Chem. 31*, 143−146.

Feng, S., Chen, J. K., Yu, H., Simon, J. A., & Schreiber, S. L. (1994) *Science 266*, 1241−1247.

Feng, S., Kasahara, C., Rickles, R., & Schreiber, S. L. (1995) *Proc. Natl. Acad. Sci. U.S.A. 92*, 12408−12415.

Goudreau, N., Cornille, F., Duchesne, M., Parker, F., Tocque, B., Garbay, C., & Roques, B. P. (1994) *Nat. Struct. Biol. 1*, 898−907.

Grzesiek, S., Bax, A., Clore, G. M., Gronenborn, A. M., Hu, J.-S., Kaufman, J., Palmer, I., Stahl, S. J., & Wingfield, P. T. (1996) *Nat. Struct. Biol. 3*, 340−345.

Guntert, P., Braun, W., & Wüthrich, K. (1991) *J. Mol. Biol. 217*, 517−530.

Kapellar, R., Prasad, K. V. S., Janssen, O., Hou, W., Schaffausen, B. S., Rudd, C. E., & Cantley, L. C. (1994) *J. Biol. Chem. 269*, 1927−1933.

Karplus, M. (1959) *J. Chem. Phys. 30*, 11−15.

Koch, C. A., Anderson, D., Moran, M. F., Ellis, C., & Pawson, T. (1991) *Science 252*, 668−674.

Kuriyan, J., & Cowburn, D. (1993) *Curr. Opin. Struct. Biol. 3*, 828−837.

Ladbury, J. E., & Chowdhry, B. Z. (1996) *Chem. Biol. 3*, 791−801.

Ladbury, J. E., Lemmon, M. A., Zhou, M., Green, J., Botfield, M. C., & Schlessinger, J. (1995) *Proc. Natl. Acad. Sci. U.S.A. 92*, 3199−3203.

Ladbury, J. E., Hennsman, M., Panayotou, G., & Campbell, I. D. (1996) *Biochemistry 35*, 11062−11069.

Lee, C.-H., Leung, B., Lemmon, M. A., Zheng, J., Cowburn, D., Kuriyan, J., & Saksela, K. (1995) *EMBO J. 14*, 5006−5015.

Lee, C.-H., Saksela, K., Mirza, U. A., Chait, B. T., & Kuriyan, J. (1996) *Cell 85*, 931−942.

Lemmon, M. A., Ladbury, J. E., Mandiyan, V., Zhou, M., & Schlessinger, J. (1994) *J. Biol. Chem. 269*, 31653−31658.

Lim, W. A. (1996) *Structure 4*, 657−659.

Lim, W. A., & Richards, F. M. (1994) *Nat. Struct. Biol. 1*, 221−225.

Lim, W. A., Richards, F. M., & Fox, R. O. (1994) *Nature 372*, 375−379.

Morton, C. J., & Ladbury, J. E. (1996) *Protein Sci. 5*, 2115−2118.

Morton, C. J., Pugh, D. J. R., Brown, E. L. J., Kahman, J. D., Renzoni, D. A. C., & Campbell, I. D. (1996) *Structure 4*, 705−714.

Musacchio, A., Saraste, M., & Wilmanns, M. (1994) *Nat. Struct. Biol. 1*, 546−551.

Nicholls, A., Sharp, K. A., & Honig, B. (1991) *Proteins: Struct., Funct., Genet. 11*, 281−296.

Noble, M. E., Musacchio, A., Saraste, M., Courtneidge, S. A., & Weirenga, R. K. (1993) *EMBO J. 12*, 2617−2624.

Pleiman, C. M., Hertz, W. M., & Cambier, J. C. (1994) *Science 263*, 1609−1612.

Rance, M., Sorensen, O. W., Bodenhausen, G., Wagner, G., Ernst, R. R., & Wüthrich, K. (1983) *Biochem. Biophys. Res. Commun. 117*, 479−485.

Ren, R., Mayer, B. J., Cicchetti, P., & Baltimore, D. (1993) *Science 259*, 1157−1161.

Rickles, R., Botfield, M. C., Weng, Z., Taylor, J., Green, O. M., Brugge, J., & Zoller (1994) *EMBO J. 13*, 5598−5604.

Rickles, R. J., Botfield, M. C., Zhou, X.-M., Henry, P. A., Brugge, J., & Zoller, M. J. (1995) *Proc. Natl. Acad. Sci. U.S.A. 92*, 10909−10913.

Siligardi, G., & Drake, A. F. (1995) *Biopolymers 37*, 281−292.

Skolnik, E. Y., Margolis, B., Mohammedi, M., Lowenstein, E., Fischer, R., Drepps, A., Ullrich, A., & Schlessinger, J. (1991) *Cell 65*, 83−90.

Sparks, A. B., Quilliam, L. A., Thorn, J. M., Der, C. J., & Kay, B. K. (1994) *J. Biol. Chem. 269*, 23853−23856.

Strickland, E. H. (1974) *CRC Crit. Rev. Biochem. 2*, 113−175.

Terasawa, H., Kohda, D., Hatanaka, H., Tsuchiya, S., Ogura, K., Nagata, K., Ishii, S., Mandiyan, V., Ullrich, A., Schlessinger, J., & Inagaki, F. (1994) *Nat. Struct. Biol. 1*, 891−897.

Viguera, A. R., Martinez, J. C., Filmanov, V. V., Mateo, P. L., & Serrano, L. (1994) *Biochemistry 33*, 2142−2150.

Waterhous, D. V., & Johnson, W. C. (1994) *Biochemistry 33*, 2121−2128.

Wiseman, T., Williston, S., Brandts, J. F., & Lin, L.-N. (1989) *Anal. Biochem. 179*, 131−137.

Wittekind, M., Mapelli, C., Farmer, B. T., Suen, K.-L., Goldfarb, V., Tsao, J., Lavoie, T., Barbacid, M., Meyers, C. A., & Mueller, L. (1994) *Biochemistry 33*, 13531−13539.

Wu, X., Knudsen, B., Feller, S. M., Zheng, J., Sali, A., Cowburn, D., Hanafusa, H., & Kuriyan, J. (1995) *Structure 3*, 215−226.

Yu, H., Chen, J. K., Feng, S., Dalgarno, D. C., Brauer, A. W., & Schreiber, S. L. (1994) *Cell 76*, 933−945.

BI9620969